Model of an Interdigitated Microsensor to Detect and Quantify Cells Flowing in a Test Chamber.

Elena Bianchi *[1,3], Federica Boschetti[1], Gabriele. Dubini[1] and Carlotta Guiducci[2]
[1]LABS, Laboratory of Biological Structure Mechanics, Structural Engineering Department, Politecnico di Milano, MI, Italy
[2]CLSE - Laboratory of Life Science Electronics - IBI, Institute of Bioengineering, IEL, Institute for Electrical Engineering, Swiss Federal Institute of Technology, EPFL, Lausanne, Switzerland
[3]Bioengineering Department, Politecnico di Milano, MI, Italy
*Corresponding author: elena3.bianchi@mail.polimi.it, LaBS – Politecnico di Milano, piazza Leonardo da Vinci 32, Milano, ITALY.

Abstract: A finite elements model of an interdigitated microsensor has been used to investigate the sensitivity of the sensor to the detection and the quantification of cells flowing in a test chamber. In particular the sensitivity of the sensor towards the geometry of sensors and the presence of a cell flowing through the channels was evaluated; several sensors topologies were considered in order to define proper guide-lines for the design of the microsensor.

Keywords: impedance spectrometry, cell counting, interdigitated electrodes

1. Introduction

Microfabricated electrodes can detect and analyze cells or particles giving a multi-frequency impedance-based characterization. The detection and/or the characterization are based on the dielectric properties of the cells coming from their membrane capacitance and conductivity, that allow to discriminate cells from their buffer solution. These properties can be also correlated to physiological differences between cells or pathological changes in cell over time. [1]
This method presents several advantages: real-time detection, label-free analysis, non-invasive sensing, easiness of integration and high-throughput screening [2]. An impedance based sensor detects the impedance change $\triangle Z$ due to the particle passing through an opening placed between two planar or facing electrodes [3,4,5,6].
Hydrodynamic techniques for focusing can be conveniently introduced to direct line of cells to the most sensitive area of the sensor [3,4,6]. In this paper we describe a numerical model of an impedance sensor, designed to quantify in real time the number of cells flowing in a micro-test adhesion chamber with a flow-section of 1.5 mm x 50 μm. Flow-rates requested in the camera can not be carried by a single sensor channel, whose dimensions should be proportional to the cells (12-17 μm), due to the high shear-stress applied on the cells in such condition of flow.
The modeling of a multiple impedance sensor combining an interdigitated design [5,7] and a vertical electrode approach [1,4] is presented in this paper. This microsensor is conceived to be integrated in a high-throughput microdevice, containing several chambers: a multiple control for each array of sensors has to be evaluated in order to achieve the simultaneous reading multiple chambers. The numerical model is designed to evaluate the performances of an array of impedance facing electrode sensors in detecting flowing cells.

2. Materials and Method

A microfabrication process to implement an array of interdigitated vertical sensors was defined: 3D structure of Si should be etched, passivated with a 200nm SiO_2 insulating layer and then selectively deposited with a metal layer (Pt – 200nm) to give rise to vertical electrodes walls. Wiring metal surfaces were passivated with a second SiO_2 deposition Hydrodynamic structures in PDMS (Polydymetilsiloxane) are located before and after the array of sensors, in order to canalize the flowing cells through the sensor gates (Fig.1). Cell population of interest are RBL (RBL-2H3 rat basophilic leucemia cells) that were represented as spheres with ∅ 15 μm, characterized by a resistive interior bulk and

a capacitive membrane, hanged in a low conductive buffer solution.

Several micro-sensor topologies and geometries (Fig.1) were investigated in order to evaluate the sensitivity of the structure to the presence of cells: W_c (width of the sensor channel), W_p (width of the pillars were the electrodes are deposed), L_c (lenght of the sensor channel). Single channel structures were compared to double channel structures in order to evaluate the feasibility of a single control on a multiple channel sensor.

An AC voltage input signal of 50 [mV] was set at several frequencies values, from 10^{-5} to 10^{9} Hz, in order to evaluate the impedance of the system as a function of input frequencies. Impedance [Ω] of the system, measured by the electrodes immersed in buffer solution, was extracted as the inverse value of admittance [S], and compared to the impedance of the system if one cell is positioned in the sensitive areas.

The consequent electrical model is showed in Fig.2. Electrical properties of materials are listed in Table 1.

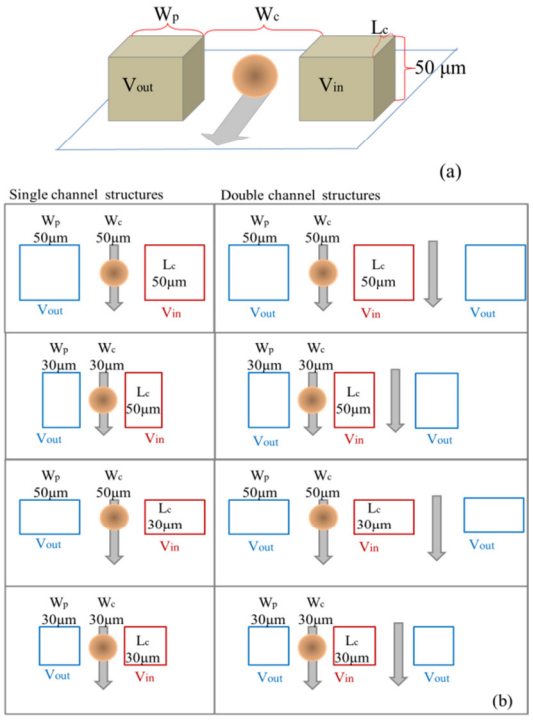

Figure 1 (a). Sketch of the sensor geometry: W_p, W_c, L_c are the three geometrical parameters that define the shape and the position of the pillars to determine the sensor channel. **(b)** Single and double channel structures tested and compared in the numerical model.

Table.1 Model parameters

	C [S/m]	ε_r [-]	d[µm]
Si [+,*]	0.1	11.7	-
SiO_2 [+]	-	4.5	0.2
Pt [*]	9.9 10^{+6}	-	-
Buffer fluid [+]	0.017	80	-
PDMS [+]	-	3.8	-
Cell membrane [8,9]	-	5.6	0.5
Cell Interior [9]	0.7	-	-
electr./solut interface [10]	2.710^{-9}	3.39 10^{-2}	0.2

*Comsol Material Library
+ Datasheet

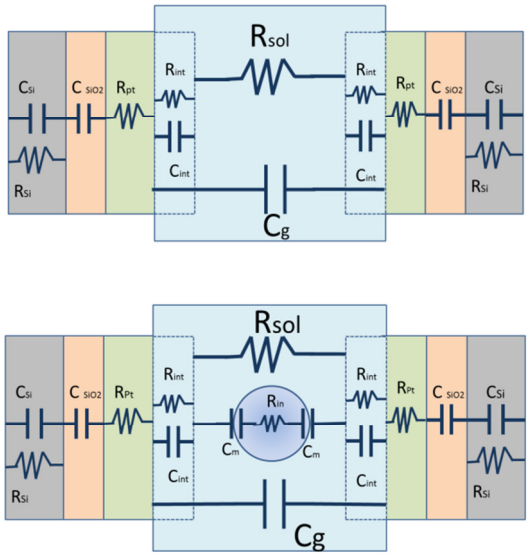

Figure 2. .Electrical model of a single couple of electrodes in absence and in presence of a cell.

R_{sol}= resistance of the buffer solution
C_g = geometrical capacitance
R_{int} = metal/solution interface resistance
C_{int}= metal/solution interface capacitance
R_{Pt} = Platinum resistance
C_{SiO2}= Silicon dioxide capacitance
R_{Si}= silicon resistance
C_{Si}= silicon capacitance
R_{in}= cell cytoplasm resistance
C_m= cellular membrane capacitance

3. Use of COMSOL Multiphysics

The model was built on Comsol platform, referring to the EC Electric Current model (1)

$$-\nabla \cdot ((\sigma + j\omega\varepsilon_0\varepsilon_r)\nabla V - \boldsymbol{J^e} = 0 \qquad (1)$$

where σ is the conductivity [S/m], ω is the frequency [Hz],ε_0 is the vacuum permittivity [8.84 10^{-12}-], ε_r the relative permittivity of the material, V the potential [V] and J^e is an external generated current density [A/m^2], defining the electric field by the constitutive law (2)

$$\boldsymbol{D} = \varepsilon_0\, \varepsilon_r\, \boldsymbol{E} \qquad (2)$$

where D is the electric displacement field and E the electric field [V].
Interface impedance, the SiO_2 thin layer and the cell membrane were represented as *contact resistances:*

$$n \cdot \mathbf{J_i} = \frac{\mathbf{1}}{\mathbf{Z_L}} (V_1 - V_2) \qquad (3)$$

defined by a thickness *d* [m] and an conductivity complex relation (4)

$$\dot{\sigma} = \sigma + j\omega\varepsilon_0\varepsilon_r \qquad (4)$$

Analyses were solved in the frequency domain, setting the parametric solver to evaluate the response of the system at several working frequencies. Input signal was given by means of a *Voltage Terminal,* and the impedance Z_f, as function of frequency, was evaluated as written out as inverse of the admittance Y.

4. Results

Impedance spectroscopy simulations were performed, in order to evaluate several geometries of single and double sensor channels, full of buffer solution. Fig.4 shows the dependence of input frequencies on R [Ohm] (in the definition of impedance Z = R+jX, R is the real term and X is the imaginary term).
Due to the presence of several capacitive contributions, two plateaus can be identified in that plot (Fig. 3): according to preliminary analytical estimations the low frequency plateau represents the high resistance of the electrodes/solution interfaces; on the other hand the high frequencies resistance plateau refers to the impedance of the solution interposed the electrodes.

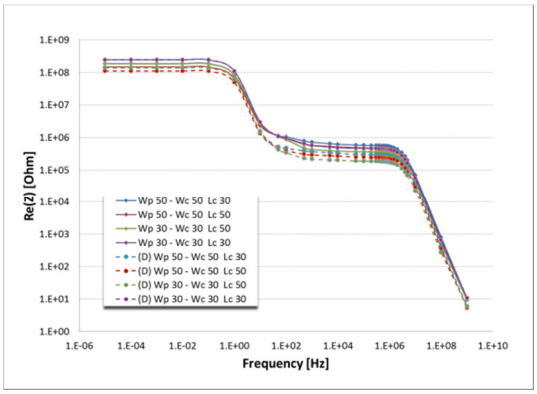

Figure 3. Resistance of the system full of steady buffer solution. Resistance is function of input AC frequencies. (D) indicates the double channel structures.

In the same condition of absence of cells a Nyquist plot (Fig.4) shows the increase of impedance as a function of the sensors geometry.

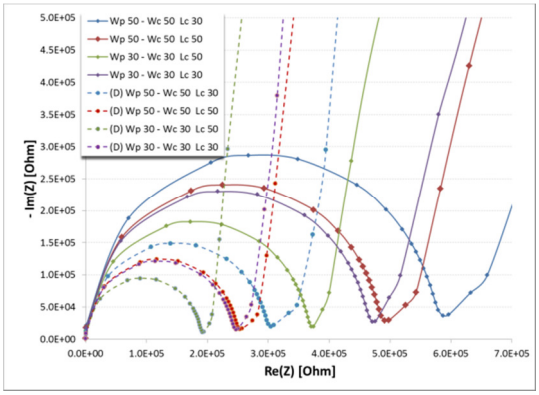

Figure 4. Nyquist plot of the different tested geometries: the frequency range from $5{\cdot}10^5$ to $1{\cdot}10^9$ Hz. (D) indicates the double channel structures.

Numerical simulations introducing a cell inside the sensor channel were performed, considering both single and double geometries. In Fig. 5 the performances of the tested geometries were plotted and compared.
The highest change on the real part of the impedance caused by the presence of the cell is attained at a frequency around $1.3{\cdot}10^6$. Double

structures show smaller perturbations caused by the cell, due to the non-negligible contribution of the second sensor channel.

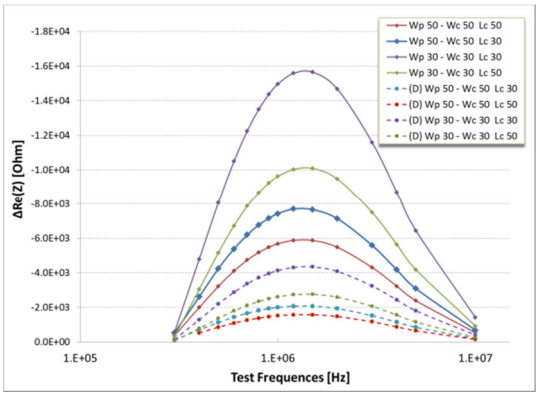

Figure 5. Portion of chart showing the decreasing of resistivity caused by the presence of a cell in the sensor channel (y axis has negative values). For each single structure, the cell is positioned in the middle of the sensor channel; (D) indicates the double channel structures.

5. Discussion

Numerical simulations of impedance spectroscopy were performed in order to evaluate the performance of a cell counter sensor made by multiple facing/interdigitated electrodes. Simulations performed on single and double structures were able to show the contributes of wire conduction, electrode/solution interfaces and passivation layer. The decrease of impedance due to the presence of cells in the sensor channels is consistently higher for single than for double channel structures. According to the simulations, the most suitable geometry for detecting the presence of cells is characterized by W_p, W_c and L_c equal to 30 μm: the coupling between the two facing electrodes is enhanced due to the smaller distance between the two metal surfaces and the shorter length of the sensor channel.

It was possible to identify an optimum observation frequency in terms of changes on the impedance in order to detect the presence of a cell in a channel. Moreover, the single channel configuration is more performant compared to the employment of two channels, though the change in impedance is not negligible.

Some effects were not considered in the present simulation such as the contribution of fluid flow inside the microchannel, and the electrical coupling of the system to the silicon platform where the micro-sensor is built on.

6. Conclusions

The problem of designing a cell counter to quantify in real-time the number of cells flowing in an adhesion microchamber with a large flow-section (1.5 mm) is approached by a numerical model built on Comsol platform.

The electrical model for the wires, passivations, electrode/solution interfaces, bulk solution and cell was defined. Simulations of impedance spectroscopy were able to highlight the contribution of the different elements depending on the frequency.

It was possible to verify that a single channel is more performant with respect to a double channel in the detection of a single cell, though the change in impedance in the latter case is not negligible.

It was also possible to identify the most suitable range of frequencies for the cell detection by impedance spectroscopy.

Four different geometries of the vertical electrodes were investigated. The best results were obtained for smallest volume of the fluid between the two facing electrodes, however, this is limited by the height of the chamber employed for cell adhesion tests.

Moreover, in order to find the minimal dimension of the channel, it is necessary to verify that the cell does not undergo any damaging mechanical stress due to the fluid dynamic conditions inside the channel.

8. References

1. K. Cheung S. Gawad, P. Renaud, Impedance spectroscopy flow cytometry: on chip label-free differentiation. *Cytometry Part A*, 65**A**, 124-132 (2005).

2. K. Cheung M. Di Berardino, G. Schade-Kapmann, M. Hebeisen, A. Pierzchalsky, J. Bocsi, A. Mittag, A. Tarnok, Microfluidic impedance-based flow cytometry, *Cytometry Part A*, **77A**, 648-666 (2010).

3. D. Holmes, T. Sun, H. Morgan J. Holloway, J. Cakebread, D. Davies, Label-free Differential Leukocyte Counts Using a Microfabricated Single-Cell Impedance Spectrometer, *IEEE SENSOR 2007, 1452-1455*

4. R. Rodriguez-Trujillo O. Castillo-Fernandez, M. Garrido, M. Arundel, A. Valencia, G. Gomila, High-speed particles detection in a micro-Coulter counter with two dimensional adjustable aperture, *Biosensors and Bioelectronics*, **24**, 290-296 (2008)

5. S. Gawad, L. Schid and Ph. Renaud, Micrmachined impedance spectroscopy flow cytometer for cell analisys and particle sizing, *Lab on chip*, **1,** 76-82, 2001.

6. T. Sun, D. Holmes, S. Gawad, N. G. Green, H. Morgan, High speed multi-frequency impedance analysis of sigle particles in a microfluidic cytometer using maximum length sequences, *Lab on a chip*, **7**, 1034-1040 (2007)

7. T. Houssin, J. Follet, E. Dei-Cas, V. Senez, Label-free analyis of water-polluting parasites by electrochemical impedance spectoscopy, *Biosensors and bioelectronics* **25,** 1122-1129 (2010)

8. R. A. Hoffman and W. Britt, Flow-System measurment of Cell Impedance Properties, *The Journal of Histochemistry and Cytochemistry*, **27 No. 1**, 234-240 1979

9.J. Yang, Y. Huang, X. Wang, X. Wang, F. Becker,P. Gascoyne, Dielectric Properties of human Leukocyte subpopulation determined by electrorotationas a cell separation criterion, *Biophysical Journal* **76**,3307-3314 (1999)

10. a. Norlin, J. Pan, C. Leygraf, Investigation on interfacial capacitance of Pt, Ti, and TiN coated electrodes by electrochemical impedance spectroscopy, *Biomolecular Engineering*, **19**, 67-71(2002)